Nano-geometry: Spherical or quasi-spherical nanoparticles?

Stanislav V. Sokolov[1], Christopher Batchelor-McAuley[1], Kristina Tschulik[1], Stephen Fletcher[2], and Richard G. Compton*[1]

[1]**Department of Chemistry, Physical and Theoretical Chemistry Laboratory, Oxford University, South Parks Road, Oxford OX1 3QZ, UK**

[2]**Department of Physical Chemistry, Loughborough University,Leicestershire,LE11 3TU, UK**

ABSTRACT

The geometry of quasi-spherical nanoparticles is investigated. The combination of SEM imaging and electrochemical methods allows sizing and characterization of the geometry of single nanoparticles.

Keywords: Nano-impacts, coulometric sizing, quasi-spherical nanoparticles, icosahedral nanoparticles.

INTRODUCTION

Nanoparticles (NPs) are synthesized in a large variety of shapes and sizes. The resultant properties can be adjusted for a given purpose and are particularly important in biomedical applications.[1,2] Traditionally spherical nanoparticles were the focus of the research, but recently quasi-spherical NPs have shown a range of advantageous properties.[3] Particular examples of non-spherical particles are nano-cubes, which show potential for hyperthermia treatment due to the larger magnetic anisotropy of a cubic structure relative to a sphere.[4] In addition quasi-spherical particles are particularly important for catalytic applications; an example is the Oxygen Reduction Reaction (ORR)[5],which is strongly influenced by the presence of Au(100) surface domains on Au nanoparticles; the greatest catalytic activity is observed for particles which deviate from spherical geometry.

Accurate sizing is crucial and a range of methods have been developed such as Transmission Electron Microscopy (TEM), Scanning Electron Microscopy (SEM), Dynamic Light Scattering (DLS) and Nanoparticle Tracking Analysis (NTA). The main advantage of electron microscopy[6] is that a readily understandable visual shape information is obtained. However the number of particles probed is generally small ($<<$ 1000 particles) and careful sample preparation is required for these techniques conducted

in vacuum. In particular particle aggregation during drying of the sample has to be avoided as far as possible. Three-dimensional information can be obtained from TEM and SEM imaging using tilt-series of images[7], but the process is time consuming and often requires complex analysis. DLS and NTA are also routinely used as first means of sizing NPs. DLS can provide information regarding the average size of the ensemble of nanoparticles but the resulting size-distribution is typically skewed towards larger particles and may strongly depend on the instrument and analytical procedure used.[8] The sample preparation is simple and analysis is performed in solution phase. The basis of the technique is the measurement of the particle diffusion coefficient which is then related to its hydrodynamic radius and as a result all shape information is lost. With a correction for anisotropic diffusion DLS has been successfully applied to size nano-rods[9,10] but applications to other geometries are yet to appear. NTA can provide information regarding *individual* particles[11] and is less affected by presence of the large particles. However the accuracy of the obtained data is strongly dependent on video capture and analysis and is strongly affected by the skill of the operator.[11]

"Nano-impacts" provide volume information for *individual* particles and given that a statistically significant number of particles are analysed, they can also supply information about the distribution of sizes, potentially leading to better understanding of the size distributions. In contrast to electron microscopy imaging, nano-impacts can be conveniently performed in the solution phase, which reduces the influence of aggregation effects. A typical experimental setup consists of a microelectrode, held at a potential which allows full oxidation or reduction of a colliding nanoparticle, leading to a spike in a chronoamperogram.The area of each spike quantifies the charge transferred to a nanoparticle and is proportional to its size. Electrochemical nano-impacts of nanoparticles have recently been demonstrated to yield accurate size information for a range of different nanoparticle systems (silver[12], gold[13], nickel[13], iron oxide[14] and organic nanoparticles[15]) and offer an attractive alternative to the more traditional sizing methods due to low cost and relative simplicity of sample preparation whilst retaining the merits of in-situ analysis. Unlike imaging techniques which typically provide a two-dimensional top view image of the particles, nano-impacts provide the number of atoms in a nanoparticle and corresponding volumetric information via the charge passed in the electrolysis of the particle.

In the following report we introduce a general geometrical analysis for quasi-spherical nano-particles and propose a joint technique of electron microscopy imaging and nano-impacts for accurate sizing of such particles. The application of this technique is demonstrated experimentally for icosahedral-shaped silver nanoparticles using nano-impacts and SEM images to show the merits of simultaneous use of the two techniques. By combining the size distributions for quasi-spherical icosahedral particles obtained through SEM imaging and nano-impacts and applying a geometric analysis we establish an accurate

description of the nanoparticles geometry and size.

1 THEORY

A nanoparticle is a solid of certain dimensions and density. Any solid of a given geometry has a set of parameters that describe it. For example a perfect sphere is fully described by its radius; if the radius is known, additional information such as volume and surface area can be immediately obtained. For the purpose of nanoparticle sizing 'spherical' approximation is often used to simplify the analysis for quasi-spherical NPs. The size distributions of particles are commonly reported in terms of the spherical radius or diameter. Geometrically this is represented by a sphere touching each of the vertices of the polyhedron. By such an approximation a nanoparticle can be described by the radius of that sphere. This geometry is shown in Figure 1 for an arbitrary solid. Importantly from the Figure 1 it is evident that the

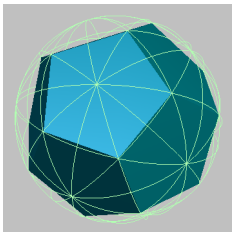

Figure 1. The Spherical approximation for an arbitrary polyhedron

volume of the sphere is larger than the volume of the original polyhedron. The ratio between the volume of the solid and circumscribed sphere is given by Equation 1 and will depend on the particular geometry of the solid. Hence the spherical approximation always results in an overestimation of the volume of a given particle. For nanoparticles the volume is dependent on the density and the number of atoms, hence an increase in volume leads to an apparent increase in the number of atoms.

$$R_{circumscribed} = \frac{V_{polygon}}{V_{circumscribedsphere}} \tag{1}$$

SEM and TEM images typically provide a two-dimensional 'flat' view of the particles. During analysis an experimantalist has to make a choice whether the particles are considered spherical or not, which is difficult for quasi-spherical nanoparticles. When considering polyhydra the degree of sphericity of a given geometric solid is defined by the isoperimetric quotient [16](IQ) as given by Equation 2, which is the ratio between the volume and the surface area.

$$IQ = 26\pi\frac{V^2}{S^3} \tag{2}$$

where V is the volume of polygon and S is the surface area. For a perfect sphere IQ=1; hence IQ is a measure of how spherical a given object is, polygons with a higher IQ will exhibit higher sphericity but that does not necessarily mean an increase in the circumscribed volume and can result in a significant overestimation in volume of the solid for some polyhedrons. Volumetric and sphericity information is shown in Figure 2 for the simple case of the five platonic solids and highlights the discrepancy between sphericity and the circumscribed volume. The general trend is that with increasing number of vertices an increase in inscribed volume is observed. However the increase in sphericity does not always correlate with the circumscribed volume as is the case for icosahedron and dodecahedron. For quasi-spherical nanoparticles the spherical approximation is insufficient for accurate characterization and size-determination.

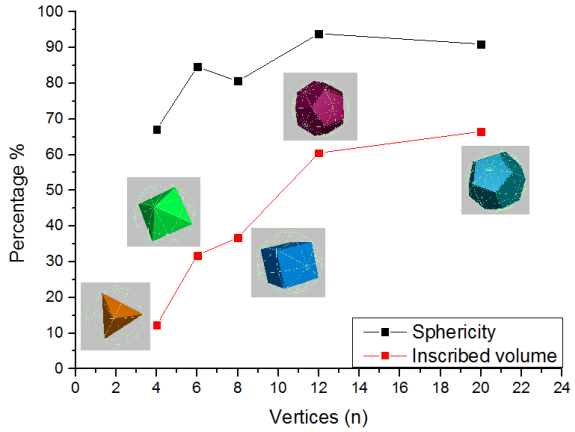

Figure 2. Relationship between the circumscribed volume and the degree of sphericity

In order to reduce such approximation error three-dimensional volumetric information is required. From nano-impacts one can obtain readily available volumetric information through the charge passed during electrolysis and use it in conjunction with electron microscopy to size particles correctly. The validity of the theory is tested experimentally for quasi-spherical silver nanoparticles in the following sections.

2 EXPERIMENTAL

2.1 Chemicals

The chemicals used were of analytical grade and purchased from Sigma Aldrich unless stated otherwise. Quasi-spherical silver nanoparticles of nominal 50 nm radius were purchased from nanoComposix as an aqueous solution. 1.4 mL of stock solution was diluted to 10 mL with a 0.1M solution of KCl for the electrochemical experiments.

2.2 Characterization via SEM imaging

The nanoparticle size and shape were characterized by using high resolution SEM imaging (SEM, LEO Gemini 1530, Zeiss).ImageJ software was used for post-processing, particle analysis and area calculations.

2.3 Electrochemical Studies

Electrochemical experiments were performed under thermostatted temperature conditions ($25 \pm 1^{\circ}$C) using a three-electrode setup with an Autolab II potentiostat (Metrohm Autolab BV, Utrecht, Netherlands). A platinum mesh was used as a counter electrode for experiments and potentials were applied relative to an SCE reference electrode (E=0.244 V vs SHE). An aqueous 0.1M KCl solution was prepared using ultrapure water (Millipore, resistivity not less than 18.2 MΩcm at 25°C). Anodic particle impacts were performed using a random array of microelectrodes (RAM) as a working electrode. A potential of 0.60 V vs SCE was chosen to ensure complete oxidation of Ag NPs.[17] A random assembly of microelectrodes[18] is an array of randomly dispersed carbon microfibers (approximately 3200 fibres) in non-conductive epoxy. Of the 3200 fibres ca 20-40% are connected[18] and each of the fibres has a radius of 3.5 micrometres. The fibres are separated by 70 micrometres from each other on average. The ends of the fibres act as individual microdisks connected in parallel. The RAM was polished before the experiments using microcloth supplied by Buehler and $0.3\mu M$ alumina particles to ensure a clean and reproducible surface. For the studies 20 chronoamperograms of 50s duration were recorded at a potential of 0.60 V vs SCE and 256 spikes were recorded in total. The resulting data was analysed using the software Signal Counter[19] (developed by Dario Omanović of the Center for Marine and Environmental Research, Ruđer Bošković Institute, POB 180, 10002 Zagreb, Croatia) to identify spikes, perform baseline correction and calculate the charge per given impact. The software Origin Pro 9.0 (Origin Lab Corporation) was used for data visualization and histogram analysis.

2.4 Diffusional weighting

Large nanoparticles have lower diffusion coefficient according to Stokes-Einstein Equation[20] 3 which leads to a lower probability of observing impact on a single microelectrode.

$$D = \frac{k_b T}{6\pi\eta r} \tag{3}$$

where k_b is Boltzmann constant, T is temperature, η is the viscosity and r is the radius of the particle. Inherent differences in diffusion coefficients needs to be taken into account during size-distribution analysis as the smaller particles have a higher probability of collision with the electrode and as a result the distribution is skewed towards smaller radius nanoparticles. Diffusion-corrected weighting[21] can be applied to the data to compensate for smaller number of larger particles being observed. The weighting is

done by calculating the midpoint diffusion coefficient for each of the bars in the histogram and dividing the resulting diffusion coefficient by the diffusion coefficient of the smallest nanoparticles. As a result individual bin count can be adjusted by the corresponding correction factor corresponding to the diffusion coefficient.

3 RESULTS AND DISCUSSION

In order to perform the geometrical analysis described in theoretical section first the SEM images were analyzed and the spherical approximation was applied in order to obtain the size distribution. In the second stage of the experiment, electrochemical sizing was performed and the resulting size distribution from volumetric data was obtained. The results were then combined and used to evaluate the geometry of the nanoparticles.

3.1 SEM image analysis

The SEM images were analysed using the ImageJ software. Automatic particle detection and particle area calculation was used. The average spherical radii ($r_{average}$) was determined according to Equation 4.

$$r_{average} = \sqrt{\frac{A}{\pi}} \tag{4}$$

where A is the area of the nanoparticle. Analysis of 55 nanoparticles showed a size range of $45 - 60$ nm in accordance with the manufacturer's specification. The size distribution shown in figure 3 has the following characteristics: the mean radius of 50 nm and the standard deviation of 4 nm. The SEM images clearly show that particles are quasi-spherical and appear to have hexagonal two dimensional projection as seen in figure 3.

3.2 Nano-impacts

Previous studies of the nano-impacts have used single microelectrodes. In the present study we used a random assembly of microfibers (RAM) with a greater surface area (1000x area of 3.5 micrometre disk). RAM allows detection of greater numbers of impacts leading to higher accuracy of particle size distribution. In addition unlike many micro-cylinder electrodes [22], arrays are robust and can be repolished multiple times. [18] A typical chronoamperogram obtained during scans is shown in Figure 4, where spikes correspond to nanoparticles-RAM collisions and spikes are not seen for blank scans in the absence of the NPs. For a given spike by integrating its area we obtain a charge of the colliding nanoparticle. If we assume that AgNPs are spherical and full oxidation takes place, then we can calculate the associated charge of a sphere with a mean radius obtained from SEM images ($r = 50$ nm). *Under a spherical approximation* the relationship between charge passed and particle's radius for $r = 50$ nm is given by

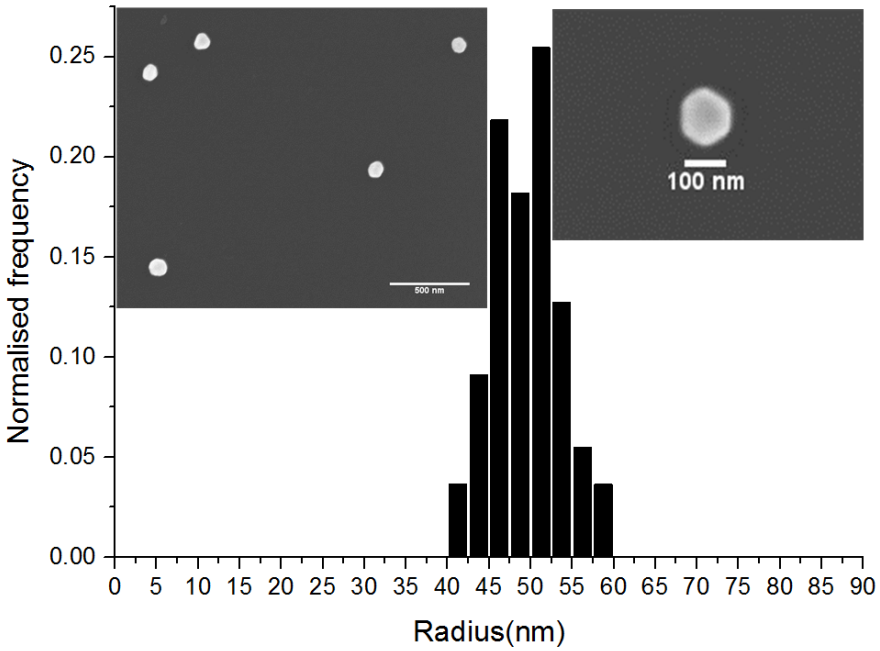

Figure 3. Size distribution of silver NPs as determined by SEM sizing

equation 5

$$Q_{expected} = \frac{8F\pi\rho r_{np}^3}{3A_r} \approx 4.9 \times 10^{-12} C \tag{5}$$

where F is the Faraday constant, ρ is the density, r is the radius of the nanoparticle and A_r is number of atoms in a nanoparticle. . From the integrated charge per spike and assuming that the particle is spherical we can calculate the corresponding radius.

256 impacts were analysed and the raw radius-distribution was obtained as a result of the above calculation. The mean experimental charge was $\approx 2.5 \times 10^{-12} C$, which is $\approx 51\%$ of the charge calculated for 50 nm perfectly spherical NP as obtained from SEM images with the spherical approximation. The mean calculated nominal radius from impact experiments is 40 nm, with a standard deviation of $10nm$. The nano-impacts experiment show consistently lower charge than anticipated for an idealised sphere with a 50 nm radius as obtained from SEM images. One possible cause of the discrepancy could be related to the diffusion of the nanoparticles.

As a result of the diffusion correction the adjusted nominal mean radius would be 41 nm with a standard deviation of 10 nm. This suggests that difference in the diffusion of the particles can not alone account for the difference in the sizes obtained from SEM imaging and nano-impacts.

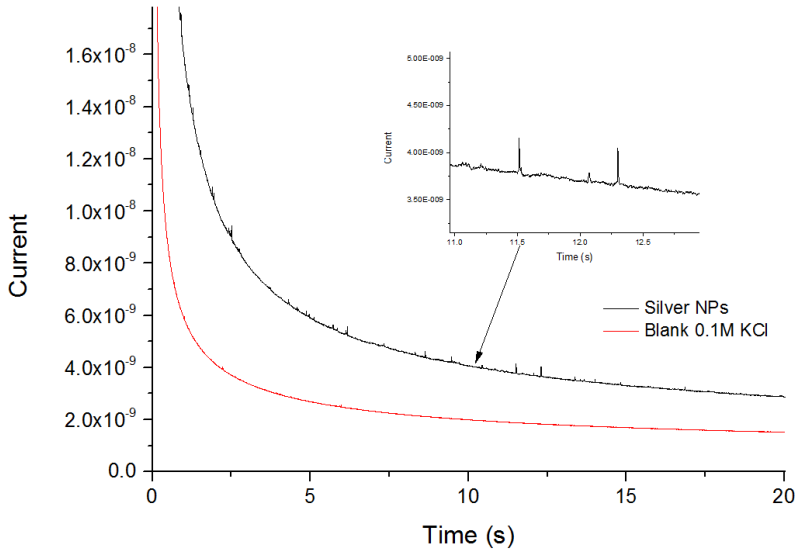

Figure 4. Chronoamperogram (black) obtained with nanoparticles present in the solution with RAM electrode and chronoamperogram (red) of blank 0.1M KCl solution without characteristic spikes

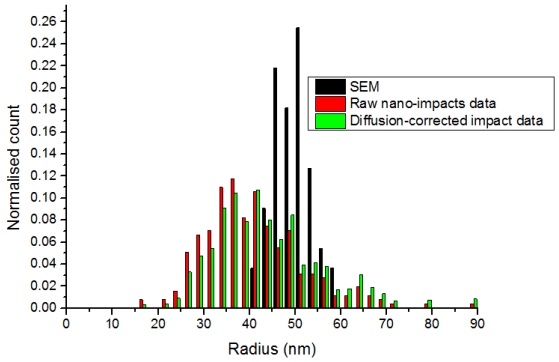

Figure 5. Comparison between size-distributions obtained from SEM and nano-impacts sizing using the spherical approximation

3.3 Geometrical considerations

The obtained size distribution from nano-impacts is consistently lower compared to SEM images as shown in figure 5. In order to account for this discrepancy we present in the following section an explanation arising from quasi-spherical shape of the particles. Based on SEM images shown in Figure 3 it is possible to introduce simplified geometry more consistent with these images. A three dimensional solid is required, which when viewed in the two dimensions corresponds to an observed hexagonal shape. An icosahedron fits such requirements. It has twelve vertices with twenty equilateral faces and it belongs to a set of platonic solids[23] and is shown in figure 2. Platonic solids are ubiquitous in nature and there are several examples of synthesized nanocubes[4] and nanotetrahedrons[24] and a whole range of nano-gold platonic solids[25]. An icosahedron is likely to lie on its face provided SEM grid surface is locally smooth and hence

when viewed from above would appear as a hexagon as shown in Figure 3. Hence icosahedron-shaped particles can account for the missing charge relative a spherical appoximation.

From the SEM images we can find the length of diagonal of the hexagon and find the edge length of an icosahedron[26]. As it can be seen from the Figure 2 diagonal is equal to the diameter of the enclosing sphere. We can also express the edge length in terms of the diagonal length and is expressed mathematically by Equation 6 .

$$a_{edge} = \frac{d}{\sqrt{\Phi^2 + 1}} \tag{6}$$

where ϕ is the golden ratio ≈ 1.61803399

The volume of icosahedron is given by equation 7

$$V = \frac{5(3+\sqrt{5})}{12} * a^3 = \frac{5(3+\sqrt{5})}{12} * (\frac{d}{\sqrt{\Phi^2 + 1}})^3 \tag{7}$$

where a is the edge length of the icosahedron

$$d_{icosahedron} = 2r_{sphere} \tag{8}$$

$$V_{icosahedroncircumscribed} = \frac{V_{icosahedron}}{V_{sphere}} \approx 60.5\% \tag{9}$$

For an icosahedron the circumscribed volume is 60.5% of a unit sphere. As a result due to a reduction in the number of atoms nano-impacts would yield the corresponding reduction in charge. Hence for icosahedron circumscribed by a sphere of a radius of 50 nm the corresponding charge would be almost 40% less than the charge for that sphere. As a result when converting charge distribution obtained from nano-impacts to radius distribution of the circumscribed sphere we need to include a correction of 40% leading to a significant increase in the determined radius. If we divide the obtained charge for the impacts by 0.605 we obtain the charge of the corresponding sphere and can calculate the corresponding radius according to Equation 5.

$$S_{icosahedron} = 5 * \sqrt{3} * a^2 \tag{10}$$

where a is the edge length The surface area of an icosahedron is given by equation 10 and hence according to the equation 2 it has the highest sphericity (IQ) of all of the platonic solids of 93.9% but there is a significant difference in inscribed volume relative to circumscribed sphere. As a result it appears almost spherical from two dimensional images which can lead to a *significant* sizing error, if an SEM imaging is

used as the only sizing technique.

As a result of the above geometric correction the mean radius obtained from nano-impacts is 48 nm and standard deviation 13 nm without diffusional correction to adjust for differences in diffusion coefficients. With additional diffusional correction the mean is found to be 49 nm and standard deviation of 13 nm. The resulting histogram is shown in Figure 6. As a result the results are in good agreement with the SEM data. Through use of electrochemical impacts additional volumetric data has been obtained which suggests that nanoparticles are indeed icosahedral.

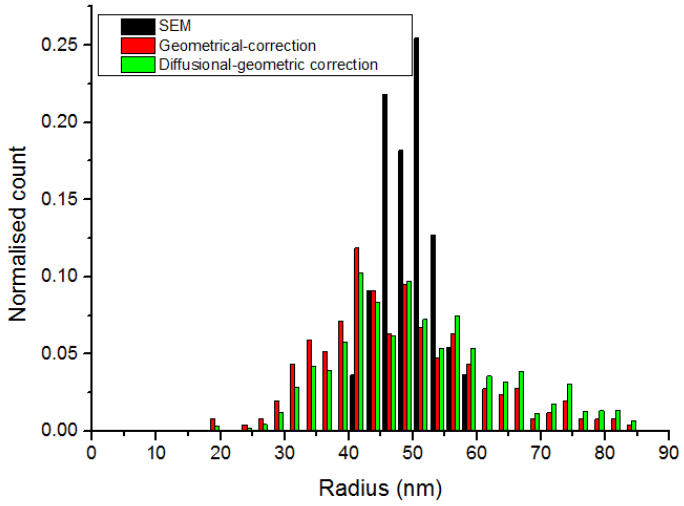

Figure 6. Normalized size distributions according to SEM imaging and nano-impacts with the applied geometric correction

4 CONCLUSIONS

In order to correctly size a given quasi-spherical particle, electron microscopy imaging is insufficient due to the inherent limitation of a two-dimensional view. Without corresponding volumetric information provided by nano-impacts the characterization is incomplete. A common pitfall in describing nanoparticle size is the use of the radius of the corresponding sphere which in many cases provides an apparent good experimental agreement but fails in the case for the example of icosahedral particles. Hence accurate sizing electron-microscopy should be ideally complemented with the electrochemical coulometric sizing technique. The above highlights the importance of the geometrical aspects of the quasi-spherical nanoparticles and allows the description of the actual shape of individual nanoparticles.

ACKNOWLEDGMENTS

The research leading to these results has received funding from the European Research Council under the European Union's Seventh Framework Programme (FP/2007-2013)/ERC Grant Agreement no. [320403].

K.T. was supported by a Marie Curie Intra European Fellowship within 7th European Community Framework Programme.

REFERENCES

[1] A. Albanese, P. Tang, and W. Chan, "The effect of nanoparticle size, shape, and surface chemistry on biological systems," *Annu. Rev. Biomed. Eng.*, vol. 14, pp. 1–16, 2012.

[2] M. Notariannia, K. Vernona, A. Choua, M. Aljadab, J. Liua, and N. Motta, "Plasmonic effect of gold nanoparticles in organic solar cells," *Sol. Energy*, vol. 106, pp. 23–37, 2014.

[3] R. Mathaes, G. Winter, A. Besheer, and J. Engert, "Non-spherical micro- and nanoparticles: fabrication, characterization and drug delivery applications," *Expert Opin. Drug Deliv.*, vol. 12, no. 3, pp. 1–12, 2014.

[4] P. Guardia, R. D. Corato, L. Lartigue, C. Wilhelm, A. Espinosa, M. Garcia-Hernandez, F. Gazeau, L. Manna, and T. Pellegrino, "Water-soluble iron oxide nanocubes with high values of specific absorption rate for cancer cell hyperthermia treatment," *ACS Nano*, vol. 6, no. 4, pp. 3080–3091, 2012.

[5] D. Uzio and G. Berhault, "Factors governing the catalytic reactivity of metallic nanoparticles," *Catalysis Reviews*, vol. 52, pp. 106–131, 2010.

[6] D. Su, *Transmission Electron Microscopy Characterization of Nanomaterials*. Springer Berlin Heidelberg, 2014.

[7] A. Kostera, U. Ziesea, A. Verkleija, A. Janssenb, J. de Graafb, J. Geusb, and K. de Jong, "Development and application of 3-dimensional transmission electron microscopy (3d-tem) for the characterization of metal-zeolite catalyst systems," *Stud. Surf. Sci. Catal*, vol. 130, pp. 329–334, 2000.

[8] B. Berne and R. Pecora, *Dynamic Light Scattering: With Applications to Chemistry, Biology, and Physics*. Dover Publications, 2000.

[9] S.Nath, C. Kaittanis, V. Ramachandran, N. Dalal, and J. Perez, "Synthesis, magnetic characterization, and sensing applications of novel dextran-coated iron oxide nanorods," *Chem. Mater*, vol. 21, pp. 1761–1767.

[10] J. Lim, D. Tan, F. Lanni, R. Tilton, and S. Majetich, "Optical imaging and magnetophoresis of nanorods," *Magn. Magn. Mater*, vol. 321, pp. 1557–1562, 2009.

[11] V. Filipe, A. Hawe, and W. Jiskoot, "Critical evaluation of nanoparticle tracking analysis (NTA) by nanosight for the measurement of nanoparticles and protein aggregates," *Pharm. Res.*, vol. 27, no. 5, pp. 796–810, 2010.

[12] Y. Zhou, N. V. Rees, and R. G. Compton, "The electrochemical detection and characterization of

silver nanoparticles in aqueous solution," *Angewandte Chemie*, vol. 50, pp. 4219–4221, 2011.

[13] Y. Zhou, E. Stuart, J. Pillay, S. Vilakazi, R. Tshikhudo, N. V. Rees, and R. G. Compton, "Electrode-nanoparticle collisions: The measurement of the sticking coefficients of gold and nickel nanoparticles from aqueous solution onto a carbon electrode," *Chem. Phys. Lett.*, vol. 551, pp. 68–71, 2012.

[14] K. Tschulik, B. Haddou, D. Omanović, N. V. Rees, and R. G. Compton, "Coulometric sizing of nanoparticles: Cathodic and anodic impact experiments open two independent routes to electrochemical sizing of fe3o4 nanoparticles," *Nano Res.*, vol. 6, no. 11, pp. 836–841, 2013.

[15] W. Cheng, X. Zhou, and R. G. Compton, "Electrochemical sizing of organic nanoparticles," *Angewandte Chemie International Edition*, vol. 52, pp. 12980–12982, 2013.

[16] G. Polya, *Induction and Analogy in Mathematics*. Princeton University Press, 1954.

[17] E. J. E. Stuart, N. V. Rees, J. T. Cullen, and R. G. Compton, "Direct electrochemical detection and sizing of silver nanoparticles in seawater media," *Nanoscale*, vol. 5, no. 174, 2013.

[18] S. Fletcher and M. D. Horne, "Random assemblies of microelectrodes (RAM electrodes) for electrochemical studies," *Electrochem. Com.*, vol. 1, pp. 502–512, 1999.

[19] J. Ellison, K. Tschulik, E. J. E. Stuart, K. Jurksch, D. Omanovic, M. Uhlemann, A. Crossley, and R. G. Compton, "Get more out of your data: A new approach to agglomeration and aggregation studies using nanoparticle impact experiments," *Chem. Open*, vol. 2, pp. 69–75, 2013.

[20] A. Einstein, "Über die von der molekularkinetischen theorie der wärme geforderte bewegung von in ruhenden flüssigkeiten suspendierten teilchen," *Annalen der Physik*, vol. 322, no. 8, pp. 549–560, 1905.

[21] J. C. Lees, J. Ellison, C. Batchelor-McAuley, K. Tschulik, C. Damm, D. Omanovic, and R. G. Compton, "Nanoparticle impacts show high-ionic-strength citrate avoids aggregation of silver nanoparticles," *Chem. Phys. Chem. Commun.*, vol. 14, pp. 3895–3897, 2013.

[22] J. Ellison, C. Batchelor-McAuley, K. Tschulik, and R. G. Compton, "The use of cylindrical microwire electrodes for nano-impact experiments; facilitating the sub-picomolar detection of single nanoparticles," *Sensor. Actuat. B-Chem*, vol. 200, no. 47-52, 2014.

[23] M. Atiyah and P. Sutcliffe, "Polyhedra in physics, chemistry and geometry," *Milan J. Math.*, vol. 71, no. 1, pp. 33–58, 2003.

[24] S. Gao, J. Yang, Z. Li, X. Jia, and Y. Chen, "Bioinspired synthesis of hierarchically micro/nano-structured cui tetrahedron and its potential application as adsorbent for cd(ii) with high removal capacity," *J. Haz. Mat.*, vol. 211-212, pp. 55–61, 2012.

[25] F. Kim, S. Connor, H. Song, T. Kuykendall, and P. Yang, "Platonic gold nanocrystals," *Angewandte Chemie International Edition*, vol. 43, pp. 3673–3677, 2004.

[26] K. J. M. MacLean, *A Geometric Analysis of the Platonic Solids and Other Semi-Regular Polyhedra (Geometric Explorations).* Loving Healing Press, 2007.